Materials Advances

ROYAL SOCIETY OF CHEMISTRY

PAPER

View Article Online
View Journal | View Issue

Check for updates

Cite this: *Mater. Adv.*, 2023, 4, 5546

Ultrasonic–biogenic synthesis of silver on anodized aluminum with superior antibacterial properties†

Henry Agbe, *[a] Dilip Kumar Sarkar,[b] X.-Grant Chen[b] and David Dodoo-Arhin[c]

Received 5th July 2023,
Accepted 9th October 2023

DOI: 10.1039/d3ma00366c

rsc.li/materials-advances

The design and fabrication of high-touch surfaces with antibacterial properties can reduce microbial burden and subsequent nosocomial infections in a hygiene critical environment. In the present study, biogenic silver nanoparticles (biogenic Ag-NPs) have been synthesized and deposited *in situ* on an anodized aluminum oxide surface using an ultrasound-assisted onion extract synthesis process. Morphological features and chemical composition have been characterized using scanning electron microscopy (SEM), energy dispersive X-ray spectroscopy (EDS), X-ray diffraction (XRD) spectroscopy, UV-Vis absorption spectroscopy and attenuated total reflection-Fourier transform infrared (ATR-FTIR) spectroscopy. The biogenic Ag-NP-coated anodized aluminum exhibited 100% *E. coli* bacteria inactivation under 60 minutes of contact.

1. Introduction

High-touch surfaces in a hygiene critical environment can serve as a reservoir for the transmission of microbial pathogens.[1] In particular, in hospital settings, the most vulnerable and immunocompromised patients are highly at risk of infections, the so-called healthcare-associated infections (HCAI) or nosocomial infections.[2] In Canada, more than 200 000 patients contract healthcare-associated infections per year, out of which 8000 cases result in fatality.[3] In the USA, more than 2 million patients contract HCAI annually, leading to about 100 000 fatalities, and a financial loss of $4.5 billion.[4] Furthermore, at any given time, up to 7% of patients in developed countries and 10% of patients in developing countries are affected by at least one HCAI.[5] Thus, HCAI has become a serious global public health problem and the 4th leading cause of death after cancer, heart disease and stroke.[3] Although hand hygiene is accepted as one of the most effective preventive methods for curbing HCAI, there is now a recognized need for novel methods such as use of disinfectants, antibiotics and engineering of touch surfaces with inherent antibacterial properties, in addition to an appropriate cleaning regime,[6] to combat HCAI.

Antibacterial surfaces, achieved by the modification of high-touch surfaces (doorknobs, bedrails and over bed tables) with antibacterial characteristics, have been recognized to be an important strategy for curbing the spread of HCAI.[7] High-touch surfaces modified with antibacterial agents such as copper, silver, triclosan and quaternary ammonium compounds are well-documented.[7] Among these, antibacterial silver nanoparticles appear interestingly attractive due to their broad-spectrum antimicrobial activity against a wide variety of pathogens such as bacteria, fungi, yeast, viruses, and protozoa.[8] In fact, the antibacterial properties of silver have been known throughout history. For example, the ancient Chaldeans used silver to heal wounds as early as 4000 B.C., before the discovery of pathogenic microbes.[9] In addition, the ancient Greeks and Romans sterilized water in silver vessels[9] and by the turn of the 20th century, silver had become the main antimicrobial agent. Nonetheless, the use of silver was limited due to its high cost of production and the discovery of penicillin by Sir Alexander Fleming in 1928.[10] However, given the high incidence of antimicrobial resistance to conventional antibiotics, presumably due to the indiscriminate use of antibiotics and mutation (leading to the development of antimicrobial resistant strains), there is an urgent need not only for alternative potent antimicrobial solutions to antibiotics but also for cheaper and more sustainable solutions to antimicrobial resistant infections associated with indwelling medical devices and high touch surfaces. In this regard, nanotechnology serves as an important toolkit for synthesizing a variety of promising antimicrobial agents such as silver nanoparticles.

[a] *Department of Materials Engineering, College of Engineering, Kwame Nkrumah University of Science and Technology, PMB University Post Office, KNUST-Kumasi, Ghana. E-mail: henry.agbe@knust.edu.gh*
[b] *Department of Applied Science, University of Québec at Chicoutimi, Aluminum Research Center – REGAL, Chicoutimi, QC, G7H 2B1, Canada*
[c] *Department of Materials Science and Engineering, University of Ghana, P.O. Box LG 77, Legon-Accra, Ghana*

† Electronic supplementary information (ESI) available. See DOI: https://doi.org/10.1039/d3ma00366c

Conventionally, silver nanoparticles (Ag-NPs) have been synthesized using physical, chemical or electrochemical reduction processes.[11] However, biological methods are emerging as an ideal alternative due to their environmental friendliness, low cost, scalability, biocompatibility, and non-toxicity among others.[12] Various microorganisms, including bacteria and fungi, and plant extracts (such as *Allium cepa*, *Cinnamomum zeylancium, Mentha aquatica* leaf, *etc.*) have been explored for the synthesis of Ag-NPs.[13] However, plant extract synthesis routes have attracted the attention of scientists in recent times due to their cost-effectiveness and simplicity (in terms of the lack of multiple processing step, compared to micro-organisms, which may require further steps such as the isolation of microbes, culture preparation, culture passage and maintenance).[14,15] Furthermore, plant extracts are inherently reducing and stabilizing agents, and possess antimicrobial, antioxidant, antidiabetic and antispasmodic properties.[16–19] Thus, biogenic Ag-NPs synthesized using plant extracts have been widely reported in the literature.[17,20–22] For instance, Gomaa[17] synthesized biogenic Ag-NPs using onion extracts as both reducing and antimicrobial agents against *Staphylococcus aureus* (*S. aureus*), *Escherichia coli* (*E. coli*) and *fungi.* In a related study by Sekar *et al.*,[18] biogenic Ag-NPs from *Allium cepa* were effective against not only foodborne illness-causing pathogens such as *Bacillus* sp., *S. aureus, Corynebacterium* sp., *E. coli and Salmonella* sp. but also *Vibrio cholera*. However, while plant extracts are ideal reducing and stabilizing agents for biogenic Ag-NP synthesis, morphology of the as-synthesized Ag-NPs is typically large and lacks control (which depends on the nature of the plant extract and the extraction techniques).[20,23] Thus, in recent times, ultrasonication technique has emerged as an interesting alternative approach for tuning the morphological features of nanoparticles.[24–26] In particular, it facilitates the formation of a homogeneously distributed stable suspension, smaller Ag-NP size, faster reaction rate, time-efficiency, cost effectiveness and tuneability.[27] Susanna *et al.*[21] used an ultrasonic–biogenic approach to synthesize spherical (5 and 30 nm) gold nanoparticles for antioxidant, antibacterial, anticancer and wound healing applications. Meanwhile, Ahmada *et al.*[28] synthesized biogenic Ag-NPs using ultrasound and cinnamon extract for antimicrobial application. Interestingly, while many studies on ultrasonic–biogenic Ag-NP powder (synthesized using plant extracts) exist in the literature, none exists for biogenic Ag-NP coatings. For high-touch surface applications, antibacterial coatings and, in particular, their stability on underlying substrates are very pertinent. To the best of our knowledge, biogenic–ultrasonic Ag-NP synthesis on anodized aluminum *via* anodization processes, which imparts antibacterial properties with strong adhesion to aluminum touch metallic surface, is yet to be reported in the literature.

In this study, an ultrasonic-onion extract reduction process has been deployed to synthesize biogenic Ag-NPs, followed by *in situ* ultra-sound assisted deposition on anodized aluminum oxide (Ag/AAO/Al). Furthermore, antibacterial performance has been validated by both Kirby Bauer disk diffusion and dry seeding assays, making Ag/AAO/Al a promising and potential solution for antibacterial aluminum touch surface application.

2. Materials and methods

2.1 Material and preparation of onion extracts

Pure silver nitrate ($AgNO_3$) and NaOH were obtained from VWR (Quebec, Canada). Bulb onion was purchased from a local store (Saguenay-Canada). 50 g of fresh onion was weighed and washed several times (10×) with a 1 : 1 ratio mixture of ethanol and deionised water. Next, the onion was chopped using a domestic blender (Hamilton Beach Professional 58870C). The finely crushed onion was then dispersed in a 500 mL Erlenmeyer flask containing 100 mL of deionized water and soaked for 24 h. The onion suspension mixture was then filtered through Whatman Number 1 filter paper to remove residual debris. Subsequently, the filtrate was boiled at 100 °C for 15 minutes to complete the extraction process. The pale-yellowish onion extract was stored at 4 °C until further use.

2.2 Ultrasonic–biogenic synthesis of silver nanoparticles

Biogenic silver nanoparticles (biogenic Ag-NPs) were prepared using a green synthesis reduction process. Briefly, a 1 : 1 volume ratio of 0.08 M $AgNO_3$ was added drop-wise to onion extract under ultrasonication (Branson 5510R-DTH, 135 W, 42 kHz) for 1.5 h. Formation of silver nanoparticles was observed with a characteristic colour change from pale yellow to brown and was confirmed using UV-Vis spectroscopy. The biogenic Ag-NPs were collected *via* centrifugation and washed 3 times with deionised water, followed by overnight drying in an electric oven (VWR).

2.3 Deposition of biogenic Ag-NPs on anodized aluminum oxide

12.5 mL of the onion extract (*Allium cepa*) was added to 15 mL of deionised water in an 80 mL beaker. 1 M NaOH was added to the above solution to adjust the pH from 6.0 to 11, while under ultrasonication (Branson 5510R-DTH, 135 W, 42 kHz). A 2.54 cm × 5.08 cm anodized AA6061-T6 alloy was then suspended in the above solution. 12.5 mL of 0.08 M $AgNO_3$ was then added drop-wise to the onion extract suspension (containing the anodized aluminum oxide (AAO/Al)) and sonicated for 1.5 h. Finally, the biogenic silver nanoparticle-coated anodized aluminum oxide (Ag-NPs/AAO/Al) was air-dried at room temperature (~25 °C) for 24 h. The anodization process was performed according to our previously described protocol.[29] Briefly, the AA6061-T6 alloy was anodized in 3 wt% H_3PO_4 (VWR) in the galvanostatic mode at a constant current density of 40 mA cm^{-2} for 120 minutes.

2.4 Sample characterization

Surface morphology and elemental composition of the biogenic silver nanoparticle-coated anodized aluminum oxide (Ag/AAO/Al) coupons were analyzed using scanning electron microscopy (SEM, JEOL JSM-6480 LV, Pleasanton, USA), equipped with energy dispersive X-ray spectroscopy (EDS). The biogenic Ag-NPs were confirmed by UV-Vis spectrophotometric analysis (Agilent 8453 UV-visible spectrophotometer). During these measurements, the Ag-NPs were diluted 10-fold, and UV-Vis absorption spectra were recorded in a 300–800 nm wavelength range with 1 nm resolution.

The crystalline structure of the biogenic Ag-NPs and the chemical composition of the coatings were further confirmed by X-ray powder diffraction (XRD) (a Bruker D8 Discover system) and attenuated total reflection-Fourier transform infrared (FTIR) spectroscopy (ATR, Agilent Technologies Cary 630 FTIR), respectively.

2.5 Antibacterial assay

2.5.1 Kirby Bauer assay. Clinically relevant bacteria, Gram positive (+), *Staphylococcus aureus* (ATCC 6538) (*S. aureus)*, and Gram-negative (−), *Escherichia coli* (ATCC 8739) *(E. coli)* and *Pseudomonas aeruginosa* (ATCC 9027) (*P. aeruginosa*) (Hardy Diagnostics), were used in this study. Bacterial cells were grown overnight from frozen (−80 °C) glycerol stock in Mueller-Hinton Broth (MHB) (Hardy Diagnostics) at 37 °C and re-inoculated into fresh MHB (37 °C) to obtain a bacterial cell density of 10^8 colony forming units (CFU) per mL at the logarithmic growth stage. Antibacterial activity was investigated using the Kirby Bauer disk diffusion assay. Briefly, bacterial inoculum was streaked gently on agar plates to obtain a bacterial lawn culture. Subsequently, 10 μL of 5 μg mL^{-1} biogenic Ag-NPs (prepared by taking 10 μL of 100 mg mL^{-1} stock biogenic Ag-NP solution and diluting to 200 mL) was dropped onto sterile 6 mm diameter Whatman filter papers. The antibacterial soaked Whatman filter papers were seeded on the agar media. Finally, these agar plates were aerobically incubated at 37 °C for 24 h. The *Zone of Inhibition* (ZOI) was then visualised and measured using a calibrated measuring instrument. All experiments were repeated in triplicate on different days with fresh bacterial cell suspensions. Mean values were calculated from a minimum of five data points. Data were analyzed by a one-way analysis of variance (ANOVA) with Tukey–Kramer multiple comparison tests. Results were considered significant at 95% confidence level ($p < 0.05$).

2.5.2 Dry seeding assay. A novel dry seeding assay was developed to mimic the near dry conditions of frequently touched surfaces in hospital settings. Briefly, 5 μL of bacterial inoculum, grown to the exponential phase (1.5×10^8 colony-forming units/millilitre (CFU mL^{-1})) in a physiological saline buffer (0.85 wt% NaCl), was seeded on a sterile $1'' \times 1''$ area of both test and control coupons. Next, coupons were incubated at ambient conditions of 25 °C and 50 ± 10% RH in cell culture plates for pre-determined contact times (0, 15, 60, 240 and 1440 minutes). Subsequently, using sterile swabs, bacteria were transferred into a 10 mL maximum recovery diluent (MRD) (ThermoFisher), followed by serial dilutions and plating on tryptic soy agar (TSA). The plates were then incubated at 37 °C for 24 h to yield countable viable bacterial colonies (30–300 colonies per plate). Positive controls were performed for $t = 0$ and $t = 4$ h to ascertain bacterial cell viability. Antibacterial efficiency was calculated from $[(A - B)/A \times 100\%$,[30] where A = CFU per cm^2 of viable bacteria on (Ag/AAO/Al) coupon and B = CFU per cm^2 of viable bacteria on the as-received aluminum coupon (control coupons)]. For quality control and reproducibility, dry seeding assay was repeated in triplicates. Data were expressed as the average ± standard deviation (SD). At least three independent experiments were performed and in duplicate on fresh bacterial cell suspension. A one-way analysis of variance (ANOVA) and Tukey's multiple comparison tests were further used to evaluate the statistical differences between sample groups. Differences were considered statistically significant for probability or $p < 0.05$.

3. Results and discussion

3.1 Deposition of Ag-NPs on anodized aluminum oxide

Fig. 1(A) shows the UV-Vis spectrum with a typical maximum absorption wavelength (λ = 400 nm) for formation of biogenic Ag-NPs.[31] This is presumably due to localized surface plasmon resonance (LSPR) phenomenon. LSPR describes a collective oscillation of biogenic Ag-NPs conducting electrons as a result of UV-Vis light absorption.[32] Similar to that mentioned in the

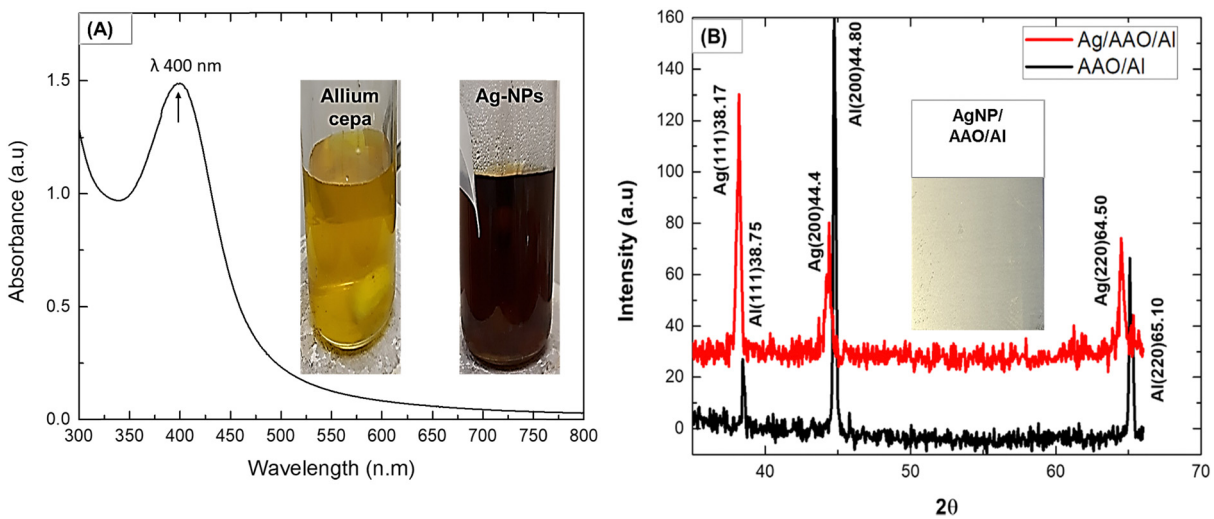

Fig. 1 UV-Vis spectrum of (A) onion extract-mediated silver nanoparticles with typical colour change from pale yellow to brown (inset); (B) XRD spectra of anodized aluminium (AAO/Al), (bottom) and biogenic Ag-NP-coated anodized aluminum (Ag/AAO/Al) (top) (inset: digital image of the Ag-NPs/AAO/Al sample).

literature,[16] the formation of biogenic Ag-NPs was characterized by a colour change from pale yellow to brown (inset in Fig. 1(A)). Notably, this colour change was observed after 1.5 h of the ultrasonic process, which signifies the complete formation of biogenic Ag-NPs. On the other hand, biogenic Ag-NP synthesis without ultrasound energy typically completes in 18–24 h.[33,34] Thus, ultrasound energy presumably catalyzed the reaction process.[35] In fact, high ultrasonic radiation (20 kHz) creates local heating effects from cavitation (formation, growth, and collapse of bubbles) to assist the nucleation and growth of biogenic Ag-NPs.[36,37] According to the theory of hot-spot mechanism, implosion of cavities (resulting from both high local temperature and cooling rate of 5000–25 000 K and $>10^{11}$ K s^{-1}, respectively), following the ultra-sonic process, leading to an increased and faster chemical reaction rate.[35] The average size of biogenic Ag-NPs was $\sim 58 \pm 25$ nm (ESI,† can be found in Fig. S1), which is consistent with the biogenic Ag-NP size range of 10–80 nm, reported in the literature.[24,28,38]

The XRD pattern, showing peaks at (111), (200) and (220) planes, corresponds to 2θ values of 38.17°, 44.31° and 64.50°,[39] respectively, and are characteristic of the silver face-centered cubic (fcc) crystal structure[39] (Fig. 1(B), top). Aluminum face-centred cubic (fcc) crystal structure with characteristic peaks at (111), (200) and (220) was also confirmed (Fig. 1(B) bottom). These peaks matched well with the JCPDS card (No. 89-3722) standard data of Ag and Al.[39] Notably, the Al peaks overlap with those of Ag, which is due to their similar lattice parameters of 0.405 nm and 0.409 nm, respectively.

The average crystallite size of biogenic Ag-NPs calculated from the Debye–Scherrer eqn (1),

$$d = \frac{K\lambda}{\beta \cos\theta} \quad (1)$$

(where, K represents the Scherrer constant (shape factor = 0.9); λ, the X-ray wavelength (1.5418 Å); β, the full width at half maximum (FWHM); and θ, the Bragg angle) was 25 nm, which is less than the particle size of 58 ± 25 nm observed for biogenic Ag-NPs, just as expected. Note that crystallite size describes dimension of individual crystalline domains whereas particle size defines individual particle's dimension within biogenic Ag-NPs.

It is well-known that $AgNO_3$ can be converted to Ag-NPs during synthesis by appropriate reducing agents.[16] Conventionly, this has been achieved using sodium borohydride, hydroquinone, photoreduction or electrochemical reduction strategies.[40] However, due to toxicity concerns, biosynthesis (mediated by biomolecules of onion extract such as flavonoid, phenol compounds and alkaloids) is favourable.[41] Hence, FTIR analysis was performed to study the chemical composition of the ultrasonic–biogenic Ag-NPs. Fig. 2(I) and (II) show the infrared spectra of active functional groups in the synthesized biogenic Ag-NPs. Notably, the intensity of bands for the biogenic Ag-NP spectrum only decreased compared to onion extract; thus, no functional groups were observable by FTIR for biogenic Ag-NPs. On the contrary, the absorption peak at the high frequency region, 3398 cm^{-1}, can be assigned to the OH, H-bonded alcohol and the phenol stretching vibration bonds

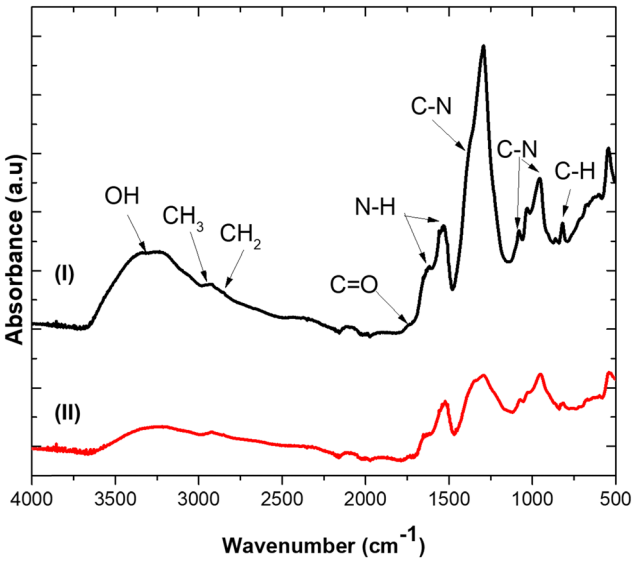

Fig. 2 ATR-FTIR spectra of (I) onion extract and (II) biogenic Ag-NPs synthesized by ultrasound and onion extract.

present in the primary, secondary amines and amide groups[42] of the onion extract. Similarly, peaks at the mid frequency region, represented as 1760 cm^{-1}, 1595–1634 cm^{-1} and 1290 cm^{-1}, can be assigned to C=O stretching in carbonyl group;[43] the N–H bending mode of primary amines; and the C–N stretching of aromatic amine groups, respectively.[17] Additionally, those at the low frequency region, representing 1047–898 cm^{-1} bands, correspond to the C–N stretching mode of alcohols, carboxylic acids, ethers and esters.[44] Finally, the 814 cm^{-1} band is attributed to the C–H stretching mode of the aromatic groups.[45]

It has been suggested that these functional groups correspond to phenols, alkaloids, tannins and terpenoid biomolecules present in onion extract that act as both reducing and stabilizing agents.[16] In particular, phenolic compounds get oxidized to quinone under alkaline conditions which provides free electrons for the reduction of Ag^+ ion to Ag^0.[24] Hence, combined effects of phenolic compounds and ultrasonic radiation resulted in biogenic Ag-NP synthesis according to the mechanism[46,47] described in eqn (2)–(9), which begins with ultrasonic mediated free radical generation, reaction cascades, nucleation and growth of biogenic Ag-NPs.

$$n\mathrm{H_2O} + \text{ultrasonic radiation} \rightarrow (\mathrm{H^*} \rightarrow \mathrm{^*OH}) \quad (2)$$

$$\mathrm{AgNO_3} \rightarrow \mathrm{Ag^+ + NO_3^-} \quad (3)$$

$$\mathrm{^*OH + RH} \rightarrow \mathrm{R^* + H_2O} \quad (4)$$

$$\mathrm{R^* + Ag^+} \rightarrow \mathrm{Ag^0 + R'' + H^+} \quad (5)$$

$$\mathrm{H^0 + Ag^+} \rightarrow \mathrm{Ag^0 + H^+} \quad (6)$$

$$\mathrm{Ag^+ + H_2O} \rightarrow \mathrm{Ag^0 + {}^*OH + H^+} \quad (7)$$

$$n\mathrm{Ag^0} \rightarrow (\mathrm{Ag^0})(\text{aggregates}) \quad (8)$$

$$(\mathrm{Ag})_n^+ \rightarrow (\mathrm{Ag})^{-1} + (\mathrm{Ag})_{(s)}^+ \quad (9)$$

The surface morphology of the biogenic Ag-NPs was studied by SEM analysis. Fig. 3(A) and (B) show the SEM micrograph of

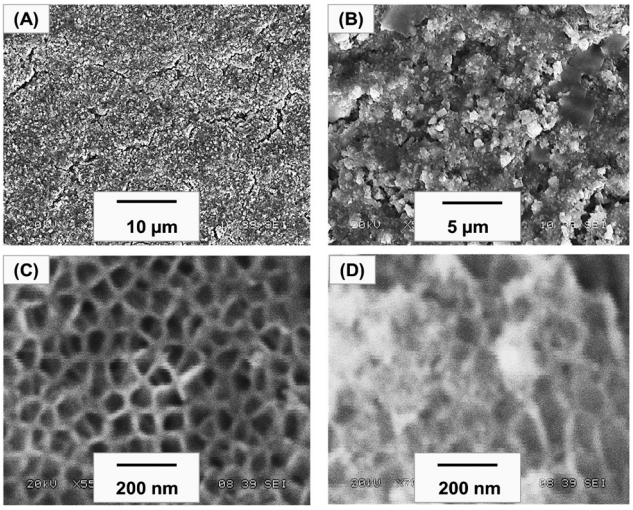

Fig. 3 SEM image of (A) and (B), the as-synthesized biogenic Ag-NPs at low (×1000) and high magnifications (×5000); (C) and (D), anodized aluminum (AAO/Al) and biogenic Ag-NP coated anodized aluminum (Ag/AAO/Al) coupon, respectively.

the as-synthesized Ag-NPs at low and high magnifications. Fig. 3(C) shows the SEM micrograph of anodized aluminum (AAO/Al), confirming the uniformly formed nano-porous structures, having average pore and cell diameters of 107 ± 24 nm and 195 ± 37 nm, respectively. In addition, nanoclusters of silver appear to be deposited *in situ* on the AAO/Al pores, as shown in Fig. 3(D). It has been suggested that shock waves and micro jet emission, occurring during cavitation (following the collapse of bubbles) enhance the physical adhesion of biogenic Ag-NPs onto solid surfaces,[48] thus the former might have promoted the injection of biogenic Ag-NPs, leading to the formation of biogenic Ag-NP-coated anodized aluminum (Ag/AAO/Al). Since the chemical nature of the biogenic Ag-NP-coated anodized aluminum is important for determining Ag^+ release, a representative portion was examined using EDS elemental mapping. Among three different locations of the elemental mapping, Fig. 4(a) shows the SEM micrograph of the representative sites, Fig. 4(b) represents the elemental EDS spectrum, comprising C, O and S with their respective Kα peaks at 0.28, 0.52 and 2.307 keV, and Lα peak of Ag at 2.98 keV. Fig. 4(c)–(g), shows the elemental mapping of Al, O, Ag, C and S respectively. Evidently, Al and O, occurring from the anodization process, covered the entire selected area (Fig. 4(c)). In addition, uniformly distributed patterns of Ag can be seen on the entire selected area (as evident in Fig. 4(e)). Also, the presence of C and S, arising from the onion extract is notable (Fig. 4(f) and (g)). Interestingly, the uniformly distributed patterns of Ag (Fig. 4(e)) could have implication for the antibacterial activity of the biogenic Ag-NP-coated anodized aluminum. In particular, the anodized pores could serve as mechanical anchorage scaffolds for holding and presumably triggering a controllable lethal dosage of Ag^+ release to kill microorganisms *via* the oligodynamic effect. Please note that Ag^+ ions of 1–10 ppm concentrations (commonly measured by inductively coupled plasma mass spectrometry (ICP-MS)) are known to impart antibacterial properties without an adverse effect on mammalian cells.[32,49] However, Ag^+ release kinetics and cytotoxic impact studies, for example, on fibroblasts cell lines, have not been carried out in the current work; these will be reported in our future contributions.

3.2 Antibacterial studies

Antibacterial performance was studied by a novel dry seeding assay and Kirby Bauer disk diffusion assay. The dry seeding assay was performed to mimic the near-dry conditions of frequently touched surfaces. The Kirby Bauer assay measures the region around the antibacterial agent where microbial growth is inhibited, the so-called ZOI. Fig. 5 shows the antibacterial performance of the tested samples.

Evidently, biogenic Ag-NPs exhibited ZOI values of 13.0 ± 1.0 mm, 11.0 ± 1.0 mm and 10.0 ± 0.9 mm against

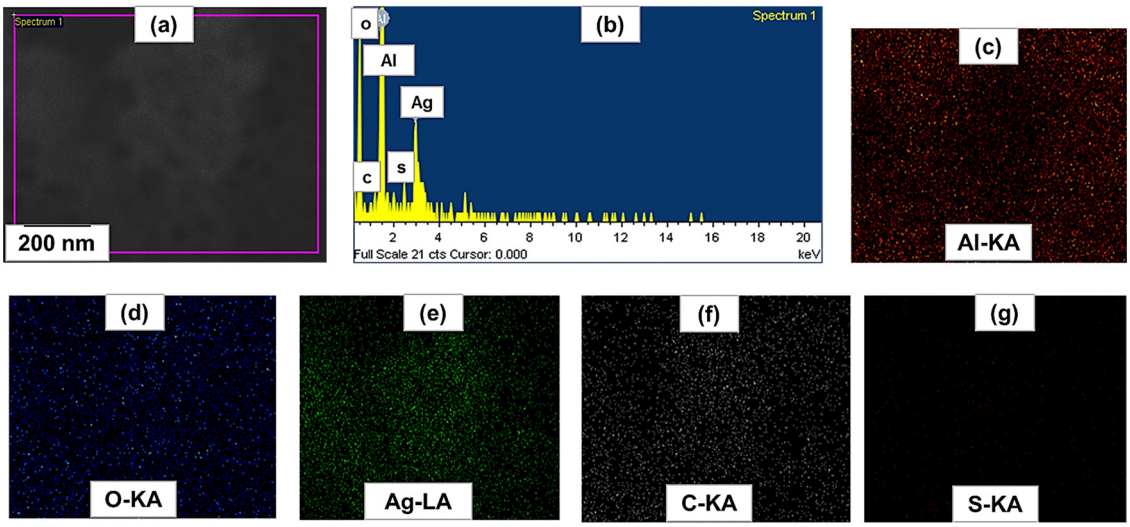

Fig. 4 SEM micrograph (a) and EDS (b), representing the selected area of biogenic Ag-NP-coated anodized aluminum (Ag/AAO/Al), respectively, and the corresponding EDS mapping of (c) Al; (d) O; (e) Ag; (f) C; and (g) S, respectively.

P. aeruginosa, S. aureus and *E. coli*, compared to onion extract, which gave a ZOI value of ~6 mm for all bacteria under study (details can be found in Table S1, ESI†). The difference in bioactivity between Gram-negative *P. aeruginosa* and Gram-positive *S. aureus* challenged against biogenic Ag-NPs may be due to the difference in cell wall composition and structure. Gram (+ve) bacteria have a thicker peptidoglycan layer (30–100 nm) composed of short peptides along with a linear polysaccharide chain cross-linking network. This rigid structure presumably inhibits the penetration of Ag-NPs. By contrast, Gram (−ve) bacteria have a relatively thinner peptidoglycan layer (2–10 nm), overlaid with an outer lipid cell membrane. Overall, it is evident that biogenic Ag-NPs are effective in inhibiting the growth of both Gram-negative and Gram-positive bacteria as demonstrated by the ZOI values. The ZOI ranging between 13 and 10 mm compares favourably with those reported in the literature. For instance, in the work of Sekar *et al.*,[18] onion extract-mediated Ag-NPs challenged against *Bacillus* sp., *S. aureus, Corynebacterium* sp., *E. coli, Salmonella* sp. and *Vibrio cholera* species resulted in ZOI ranging between 5 and 15 mm. Similarly, in the work of K. Devasvaran *et al.*,[22] microwave-assisted biogenic Ag-NPs resulted in ZOI values of 11.33 ± 0.58 mm and 12.00 ± 1.00 mm for *E. coli* and *S. aureus*, respectively. However, direct comparison of different reported results must be treated with caution, as differences may arise owing to experimental conditions.

In general, silver nanoparticles are an effective antimicrobial agent and have (1) broad spectrum antibacterial properties, with a high chemotherapeutic ratio;[50] (2) non-toxicity to human cells at low concentrations (10 ppm (0.01 mg mL^{-1}));[51] (3) multifunctional antimicrobial mechanism;[52] (4) strong oligo dynamic effects (especially against "super-bugs"); and (5) low tendency for antimicrobial resistance.[51,53,54] However, despite its long history as an antimicrobial agent, its actual mechanism is still unclear.[55] However, scientists agree that the oxidization of biogenic Ag-NPs by respiratory enzymes converts them into ionic silver (Ag^+).[56] Once Ag^+ ions are released, they interact with the bacterial cell wall structure, ultimately inhibiting cell wall synthesis and subsequent bacterial death.[56] What is more, Ag^+ within the cytoplasmic membrane can induce cellular damage through multiple pathways such as destabilisation of ribosome and inhibition of protein synthesis[57] or oxidative stress, releasing reactive oxygen species (ROS), which can interfere with the normal physiology of purine and pyrimidine base pairs, thus leading to the destruction of deoxyribonucleic acid (DNA) and subsequent cell death.[56,58]

To mimic the near dry conditions of real-life, we have developed a facile "dry seeding" approach to study the antibacterial properties of Ag/AAO/Al, as a potential antibacterial technology for touch surface applications. Test coupons were inoculated with *E. coli* inoculum under ambient conditions of 25 °C and relative humidity of 50 ± 10% in a cell culture plate for pre-determined contact times (0, 15, 60, 240 and 1440 minutes). Note that only Gram-negative *E. coli* was studied here since it was more resistant to biogenic Ag-NP compared to *S. aureus* and *P. aeruginosa* when studied using the Kirby Bauer disk diffusion assay (Fig. 5). Thus, a higher antibacterial activity of biogenic Ag-NP-coated anodised aluminum (Ag/AAO/Al) is expected against *S. aureus* and *P. aeruginosa*, compared to *E-coli*, similar to the observation reported in the literature.[59–61] Fig. 6(a) and (b) show the graphical representation of the antibacterial performance and schematic of sequence of the dry seeding process, respectively. Notably, Ag/AAO/Al was most effective compared to both positive control (copper, onion extract and AAO/Al) and the negative control (as-received Al). In particular, 29% of *E. coli* bacteria were killed after 15 minutes of contact with Ag/AAO/Al, compared to 15% for copper, 10% for onion extract-coated anodized aluminum (O.E./AAO/Al), 5% for anodized aluminum (AAO/Al) and 0% for the as-received aluminum. However, at 60 minutes of contact, 100% *E. coli* had been killed by Ag/AAO/Al, copper and the other controls, except the as-received aluminum, which resulted in only 12% death of *E. coli*. Thus, Ag/AAO/Al compares favourably with the results of our previous contributions[30,62] and commercially available antimicrobial copper-alloy. It should be mentioned that the United States of America's Environmental Protection Agency (EPA) has approved the registration of antimicrobial copper-alloy as "antimicrobial materials" with public health benefits and as a standard for comparing other antimicrobial touch surfaces.[63–66]

Evidently, AAO/Al also resulted in significant *E. coli* bacteria killing after 60 min of contact. This can be attributed to the nano-porous structures (pore diameter,107 ± 24 nm and cell diameter 195 ± 37 nm) achieved by the anodization process, similar to those reported for antibacterial cicada wings.[67,68] However, the antibacterial mechanism of anodized aluminum is not provided here; this will be reported in our future contribution. In contrast to Ag/AAO/Al, *E. coli* survived quite

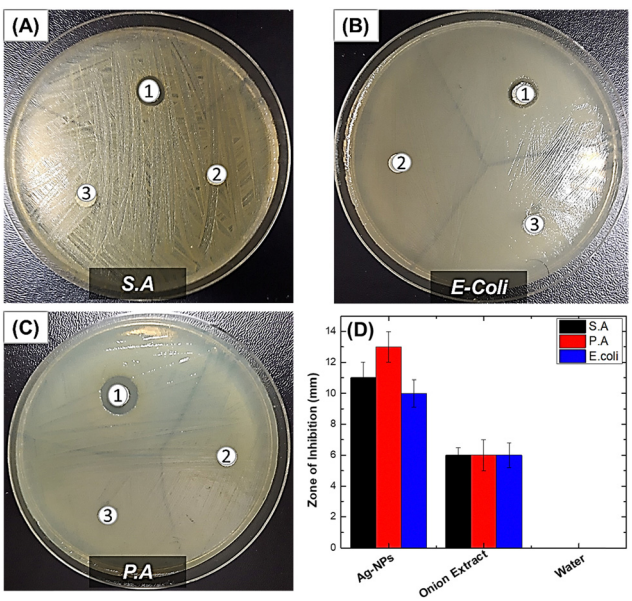

Fig. 5 Antibacterial activity of biogenic Ag-NPs and *Allium cepa* against (A) *S. aureus*, (B) *E. coli*, and (C) *P. aeruginosa*, and (D) graphical representation of ZOI. Region 1 (biogenic Ag-NPs); Region 2 (*Allium cepa*); Region 3 (distilled water—negative control). The results are the mean ± SD of 3 independent experiments performed in triplicate.

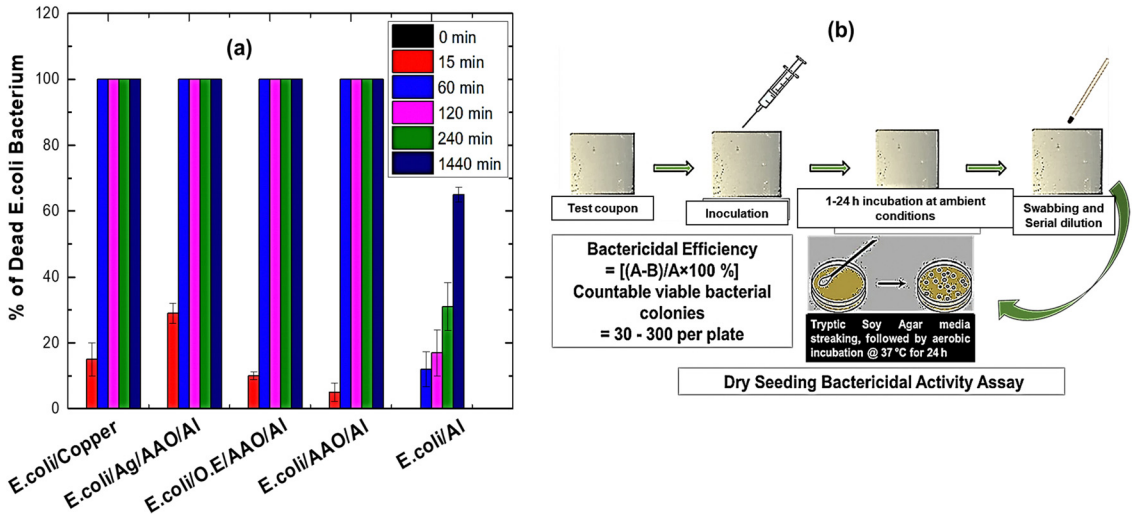

Fig. 6 Graphical representation of the antibacterial performance of biogenic Ag-NP-coated anodized aluminum (Ag/AAO/Al) compared to controls (a); and schematic of sequence of the dry seeding process (b). Error bars represent SD (standard deviations) of 3 independent experiments performed in triplicate.

well on the as-received aluminum and, after 1440 min of contact, ~35% of bacteria were still present (ESI,† can be found in Table S2). This is worrisome as such surfaces could serve as a reservoir for the spread of bacterial infection. Note that multi-drug resistant (MDR) pathogens such as methicillin-resistant *S. aureus* (MRSA), *E coli*, and *P. aeruginosa* can survive on inanimate dry high-touch surface for days, weeks or even months.[69–71] Overall, designing high-touch surfaces with inherent antibacterial properties could presumably reduce both microbial burden and nosocomial infections in a hygiene critical environment.

4. Conclusions

In this study, the ultrasonic-onion extract reduction process has been deployed to synthesize biogenic Ag-NPs, followed by *in situ* ultra-sound assisted deposition on anodized aluminum oxide. The as-synthesized biogenic Ag-NPs were effective in inhibiting the growth of clinically relevant pathogens such as *Staphylococcus aureus* (Gram +ve), *Pseudomonas aeruginosa* (Gram −ve) and *Escherichia coli* (Gram −ve) with corresponding zone of inhibition values of 11.0 ± 1.0 mm; 13.0 ± 1.0 mm and 10.0 ± 0.9 mm, respectively. Furthermore, biogenic Ag-NP-coated anodized aluminum exhibited 100% *E. coli* bacteria killing under 60 minutes of contact. These results, thus, demonstrate that the biogenic Ag-NP-coated anodized aluminum has potential for use as an antibacterial surface technology in commonly touched areas in hygiene critical environments.

Author contributions

H. A.: conceptualization, formal analysis, and writing—original draft preparation; D. K. S. conceptualization, writing—review and editing, and supervision; X. G. C.: conceptualization, writing—review and editing, and supervision. D. D. A: writing—review and editing. All authors have read and agreed to the published version of the manuscript.

Conflicts of interest

The authors declare no competing financial interest.

Acknowledgements

Authors acknowledge the financial support from Fonds de recherche du Québec – Nature et technologies (FRQNT) under the grant number 2018-LU-210883. Authors also thank Prof. Nathalie Faucheux, Prof. Gervais Soucy and Ms Jessica Jann, Department of Chemical Engineering and Biotechnology Engineering, University of Sherbrooke, for the discussion leading to the development of the novel dry seeding protocols.

References

1 C. E. Edmiston Jr, M. Spencer, B. D. Lewis, P. J. Rossi, K. R. Brown, M. Malinowski, G. R. Seabrook and D. Leaper, Assessment of a novel antimicrobial surface disinfectant on inert surfaces in the intensive care unit environment using ATP-bioluminesence assay, *Am. J. Infect. Control*, 2020, **48**(2), 143–146.
2 M. Schmidt, The role of antimicrobial surfaces in hospitals to reduce healthcare-associated infections (HAIs), *Decontamination in Hospitals and Healthcare*, Elsevier, 2020, pp. 259–299.
3 A. MacLaurin, K. Amaratunga, C. Couris, C. Frenette, R. Galioto, G. Hansen, J. Happe, K. Neudorf, L. Pelude and C. Quach, Measuring and Monitoring Healthcare-Associated Infections: A Canadian Collaboration to Better Understand the Magnitude of the Problem, *Healthcare Quart.*, 2020, **22**(SP), 116.
4 W. H. Organization, *Report on the burden of endemic health care-associated infection worldwide*, 2011.

5 W. H. Organization, *Guidelines on core components of infection prevention and control programmes at the national and acute health care facility level*, 2016.
6 M. Cole, Exploring the hand hygiene competence of student nurses: a case of flawed self assessment, *Nurse Educ. Today*, 2009, **29**(4), 380–388.
7 G. Borkow, *Use of biocidal surfaces for reduction of healthcare acquired infections*, Springer, 2014.
8 J. Boateng, *Therapeutic dressings and wound healing applications*. John Wiley & Sons, 2020.
9 W. R. Hill and D. M. Pillsbury, *Argyria: the pharmacology of silver*, Williams & Wilkins Company, 1939.
10 P. Kowalczyk, M. Szymczak, M. Maciejewska, Ł. Laskowski, M. Laskowska, R. Ostaszewski, G. Skiba and I. Franiak-Pietryga, All That Glitters Is Not Silver—A New Look at Microbiological and Medical Applications of Silver Nanoparticles, *Int. J. Mol. Sci.*, 2021, **22**(2), 854.
11 V. K. Sharma, R. A. Yngard and Y. Lin, Silver nanoparticles: green synthesis and their antimicrobial activities, *Adv. Colloid Interface Sci.*, 2009, **145**(1–2), 83–96.
12 S. Ahmed, M. Ahmad, B. L. Swami and S. Ikram, A review on plants extract mediated synthesis of silver nanoparticles for antimicrobial applications: a green expertise, *J. Adv. Res.*, 2016, **7**(1), 17–28.
13 S. Baker, A. Pasha and S. Satish, Biogenic nanoparticles bearing antibacterial activity and their synergistic effect with broad spectrum antibiotics: Emerging strategy to combat drug resistant pathogens, *Saudi Pharm. J.*, 2017, **25**(1), 44–51.
14 K. Kalishwaralal, V. Deepak, S. Ram Kumar Pandian, M. Kottaisamy, S. Barathmanikanth, B. Kartikeyan and S. Gurunathan, Biosynthesis of silver and gold nanoparticles using Brevibacterium casei, *Colloids Surf., B*, 2010, **77**(2), 257–262.
15 Y. Park, A new paradigm shift for the green synthesis of antibacterial silver nanoparticles utilizing plant extracts, *Toxicol. Res.*, 2014, **30**(3), 169–178.
16 N. Tarannum and Y. K. Gautam, Facile green synthesis and applications of silver nanoparticles: a state-of-the-art review, *RSC Adv.*, 2019, **9**(60), 34926–34948.
17 E. Z. Gomaa, Antimicrobial, antioxidant and antitumor activities of silver nanoparticles synthesized by Allium cepa extract: a green approach, *J. Genet. Eng. Biotechnol.*, 2017, **15**(1), 49–57.
18 R. K. Sekar, A. Sridhar, B. Perumalsamy, D. B. Manikandan and T. Ramasamy, In Vitro Antioxidant, Antipathogenicity and Cytotoxicity Effect of Silver Nanoparticles Fabricated by Onion (Allium cepa L.) Peel Extract, *Bionanoscience*, 2019, 1–14.
19 Y. M. Heikal, N. A. Şuţan, M. Rizwan and A. Elsayed, Green synthesized silver nanoparticles induced cytogenotoxic and genotoxic changes in Allium cepa L. varies with nanoparticles doses and duration of exposure, *Chemosphere*, 2020, **243**, 125430.
20 C. Hano and B. H. Abbasi, *Plant-based green synthesis of nanoparticles: Production, characterization and applications*, MDPI, 2021, vol. 12, p. 31.
21 D. Susanna, R. M. Balakrishnan and J. P. Ettiyappan, Ultrasonication-assisted green synthesis and characterization of gold nanoparticles from Nothapodytes foetida: An assessment of their antioxidant, antibacterial, anticancer and wound healing potential, *J. Drug Delivery Sci. Technol.*, 2023, 104740.
22 K. Devasvaran, B. Alallam, M. A. Yunus, F. R. P. Dewi, N. N. S. N. M. Kamal and V. Lim, Microwave-assisted green synthesis of silver nanoparticles using alkaline extracted crude polysaccharide of C. Nutans: Optimisation, characterisation, toxicity, anticancer potential and antibacterial studies, *J. Drug Delivery Sci. Technol.*, 2023, 104688.
23 D. Lahiri, M. Nag, H. I. Sheikh, T. Sarkar, H. A. Edinur, S. Pati and R. R. Ray, Microbiologically-synthesized nanoparticles and their role in silencing the biofilm signaling cascade, *Front. Microbiol.*, 2021, **12**, 636588.
24 A. Nouri, M. T. Yaraki, A. Lajevardi, Z. Rezaei, M. Ghorbanpour and M. Tanzifi, Ultrasonic-assisted green synthesis of silver nanoparticles using Mentha aquatica leaf extract for enhanced antibacterial properties and catalytic activity, *Colloid Interface Sci. Commun.*, 2020, **35**, 100252.
25 T. Sreekanth, P. Nagajyothi, P. Muthuraman, G. Enkhtaivan, S. Vattikuti, C. Tettey, D. H. Kim, J. Shim and K. Yoo, Ultrasonication-assisted silver nanoparticles using Panax ginseng root extract and their anti-cancer and antiviral activities, *J. Photochem. Photobiol., B*, 2018, **188**, 6–11.
26 M. S. Jameel, A. A. Aziz, M. A. Dheyab, B. Mehrdel and P. M. Khaniabadi, Rapid sonochemically-assisted green synthesis of highly stable and biocompatible platinum nanoparticles, *Surf. Interfaces*, 2020, **20**, 100635.
27 M. H. Islam, M. T. Paul, O. S. Burheim and B. G. Pollet, Recent developments in the sonoelectrochemical synthesis of nanomaterials, *Ultrason. Sonochem.*, 2019, **59**, 104711.
28 A. Ahmad, Z. Mushtaq, F. Saeed, M. Afzaal and E. Al Jbawi, Ultrasonic-assisted green synthesis of silver nanoparticles through cinnamon extract: biochemical, structural, and antimicrobial properties, *Int. J. Food Prop.*, 2023, **26**(1), 1984–1994.
29 H. Agbe, D. K. Sarkar, X. G. Chen, N. Faucheux, G. Soucy and J.-L. Bernier, Silver-polymethylhydrosiloxane nanocomposite coating on anodized aluminum with superhydrophobic and antibacterial properties, *ACS Appl. Bio Mater.*, 2020, **3**(7), 4062–4073.
30 H. Agbe, D. K. Sarkar and X.-G. Chen, Anodized Aluminum Surface with Topography-Mediated Antibacterial Properties, *ACS Biomater. Sci. Eng.*, 2022, **8**(3), 1087–1095.
31 Y. Wu, X. Sun, S. Dai, M. Li, L. Zheng, Q. Wen, B. Tang, D.-Q. Yun and L. Xiao, Broad-Band-Enhanced Plasmonic Perovskite Solar Cells with Irregular Silver Nanomaterials, *ACS Appl. Mater. Interfaces*, 2022, **14**(14), 16269–16278.
32 L. Wei, J. Lu, H. Xu, A. Patel, Z.-S. Chen and G. Chen, Silver nanoparticles: synthesis, properties, and therapeutic applications, *Drug Discovery Today*, 2015, **20**(5), 595–601.
33 M. A. Khalilzadeh and M. Borzoo, Green synthesis of silver nanoparticles using onion extract and their application for the preparation of a modified electrode for determination of ascorbic acid, *J. Food Drug Anal.*, 2016, **24**(4), 796–803.

34 T. Khan, M. A. Khan and A. Nadhman, Synthesis in plants and plant extracts of silver nanoparticles with potent antimicrobial properties: current status and future prospects, *Appl. Microbiol. Biotechnol.*, 2015, **99**(23), 9923–9934.
35 K. S. Suslick, The chemical effects of ultrasound, *Sci. Am.*, 1989, **260**(2), 80–87.
36 N. N. Nam, T. L. Bui, S. J. Son and S. W. Joo, Ultrasonication-Induced Self-Assembled Fixed Nanogap Arrays of Monomeric Plasmonic Nanoparticles inside Nanopores, *Adv. Funct. Mater.*, 2019, **29**(12), 1809146.
37 S. Valange; G. Chatel; P. N. Amaniampong; R. Behling and F. Jérôme, Ultrasound-Assisted Synthesis of Nanostructured Oxide Materials: Basic Concepts and Applications to Energy, *Advanced Solid Catalysts for Renewable Energy Production*, IGI Global, 2018, pp. 177–215.
38 V. Sekar, C. Balakrishnan, P. Kathirvel, S. Swamiappan, M. A. Alshehri, S. Sayed and C. Panneerselvam, Ultrasonication-enhanced green synthesis of silver nanoparticles using Barleria buxifolia leaf extract and their possible application, *Artif. Cells, Nanomed., Biotechnol.*, 2022, **50**(1), 177–187.
39 K. Shameli, M. B. Ahmad, A. Zamanian, P. Sangpour, P. Shabanzadeh, Y. Abdollahi and M. Zargar, Green biosynthesis of silver nanoparticles using Curcuma longa tuber powder, *Int. J. Nanomed.*, 2012, **7**, 5603.
40 E. I. Alarcon, M. Griffith and K. I. Udekwu, *Silver nanoparticle applications*, 2015.
41 P. Singh and S. K. Jain, Biosynthesis of Nanomaterials: Growth and Properties, *Rev. Adv. Sci. Eng.*, 2014, **3**(3), 231–238.
42 D. E. Zoutman, B. D. Ford, E. Bryce, M. Gourdeau, G. Hébert, E. Henderson, S. Paton, H. Canada, C. H. E. Committee and C. N. I. S. Program, The state of infection surveillance and control in Canadian acute care hospitals, *Am. J. Infect. Control*, 2003, **31**(5), 266–273.
43 P. Kalainila and V. Subha, Ernest Ravindran, R.; Sahadevan, R., Synthesis and characterization of silver nanoparticle from Erythrina indica, *Asian J. Pharm. Clin. Res.*, 2014, **7**(2), 39–43.
44 A. M. Awwad, N. M. Salem and A. O. Abdeen, Green synthesis of silver nanoparticles using carob leaf extract and its antibacterial activity, *Int. J. Ind. Chem.*, 2013, **4**(1), 29.
45 M. N. Lakhan, R. Chen, A. H. Shar, K. Chand, A. H Shah, M. Ahmed, I. Ali, R. Ahmed, J. Liu, K. Takahashi and J. Wang, Eco-friendly green synthesis of clove buds extract functionalized silver nanoparticles and evaluation of antibacterial and antidiatom activity, *J. Microbiol. Methods*, 2022, **173**, 105934.
46 M. Faried, K. Shameli, M. Miyake, A. Hajalilou, A. Zamanian, Z. Zakaria, E. Abouzari-Lotf, H. Hara, N. B. B. Ahmad Khairudin and M. F. Binti Mad Nordin, A green approach for the synthesis of silver nanoparticles using ultrasonic radiation's times in sodium alginate media: characterization and antibacterial evaluation, *J. Nanomater.*, 2016, **2016**, 4941231.
47 J. Madhavan, J. Theerthagiri, D. Balaji, S. Sunitha, M. Y. Choi and M. Ashokkumar, Hybrid advanced oxidation processes involving ultrasound: An overview, *Molecules*, 2019, **24**(18), 3341.
48 I. Perelshtein, G. Applerot, N. Perkas, G. Guibert, S. Mikhailov and A. Gedanken, Sonochemical coating of silver nanoparticles on textile fabrics (nylon, polyester and cotton) and their antibacterial activity, *Nanotechnology*, 2008, **19**(24), 245705.
49 B. Menagen, R. Pedahzur and D. Avnir, Sustained release from a metal-Analgesics entrapped within biocidal silver, *Sci. Rep.*, 2017, **7**(1), 4161.
50 J. Schierholz, L. Lucas, A. Rump and G. Pulverer, Efficacy of silver-coated medical devices, *J. Hosp. Infect.*, 1998, **40**(4), 257–262.
51 A. Gao, R. Hang, X. Huang, L. Zhao, X. Zhang, L. Wang, B. Tang, S. Ma and P. K. Chu, The effects of titania nanotubes with embedded silver oxide nanoparticles on bacteria and osteoblasts, *Biomaterials*, 2014, **35**(13), 4223–4235.
52 P. Singha, J. Locklin and H. Handa, A review of the recent advances in antimicrobial coatings for urinary catheters, *Acta Biomater.*, 2017, **50**, 20–40.
53 S. Mei, H. Wang, W. Wang, L. Tong, H. Pan, C. Ruan, Q. Ma, M. Liu, H. Yang, L. Zhang, Y. Cheng, Y. Zhang, L. Zhao and P. K. Chu, Antibacterial effects and biocompatibility of titanium surfaces with graded silver incorporation in titania nanotubes, *Biomaterials*, 2014, **35**(14), 4255–4265.
54 H. Qin, H. Cao, Y. Zhao, G. Jin, M. Cheng, J. Wang, Y. Jiang, Z. An, X. Zhang and X. Liu, Antimicrobial and osteogenic properties of silver-ion-implanted stainless steel, *ACS Appl. Mater. Interfaces*, 2015, **7**(20), 10785.
55 J. Prakash, S. Sun, H. C. Swart and R. K. Gupta, Noble metals-TiO2 nanocomposites: From fundamental mechanisms to photocatalysis, surface enhanced Raman scattering and antibacterial applications, *Appl. Mater. Today*, 2018, **11**, 82–135.
56 S. L. Banerjee, P. Potluri and N. K. Singha, Antimicrobial cotton fibre coated with UV cured colloidal natural rubber latex: A sustainable material, *Colloids Surf., A*, 2019, **566**, 176–187.
57 J.-Y. Maillard and P. Hartemann, Silver as an antimicrobial: facts and gaps in knowledge, *Crit. Rev. Microbiol.*, 2013, **39**(4), 373–383.
58 K.-H. Wu, J.-C. Wang, J.-Y. Huang, C.-Y. Huang, Y.-H. Cheng and N.-T. Liu, Preparation and antibacterial effects of Ag/AgCl-doped quaternary ammonium-modified silicate hybrid antibacterial material, *Mater. Sci. Eng., C*, 2019, **98**, 177–184.
59 M. Calovi, B. Furlan, V. Coroneo, O. Massidda and S. Rossi, Facile route to effective antimicrobial aluminum oxide layer realized by co-deposition with silver nitrate, *Coatings*, 2021, **12**(1), 28.
60 F. Russo, B. Furlan, M. Calovi, O. Massidda and S. Rossi, Silver-based vitreous enamel coatings: Assessment of their antimicrobial activity towards Escherichia coli and Staphylococcus aureus before and after surface degradation, *Surf. Coat. Technol.*, 2022, **445**, 128702.
61 J. Jann, O. Drevelle, X. G. Chen, M. Auclair-Gilbert, G. Soucy, N. Faucheux and L.-C. Fortier, Rapid antibacterial activity of

anodized aluminum-based materials impregnated with quaternary ammonium compounds for high-touch surfaces to limit transmission of pathogenic bacteria, *RSC Adv.*, 2021, **11**(60), 38172–38188.

62 H. Agbe, D. K. Sarkar and X. G. Chen, Electrochemically synthesized silver phosphate coating on anodized aluminum with superior antibacterial properties, *Surf. Coat. Technol.*, 2021, **428**, 127892.

63 J. M. Boyce, Environmental contamination makes an important contribution to hospital infection, *J. Hosp. Infect.*, 2007, **65**, 50–54.

64 H. Palza, M. Nuñez, R. Bastías and K. Delgado, In situ antimicrobial behavior of materials with copper-based additives in a hospital environment, *Int. J. Antimicrob. Agents*, 2018, **51**(6), 912–917.

65 M. Schmidt, *Copper surfaces in the ICU reduced the relative risk of acquiring an infection while hospitalized*, BMC proceedings, BioMed Central, 2011, p. O53.

66 S. L. Warnes, C. J. Highmore and C. W. Keevil, Horizontal transfer of antibiotic resistance genes on abiotic touch surfaces: implications for public health, *mBio*, 2012, **3**(6), e00489.

67 J. Hasan, H. K. Webb, V. K. Truong, S. Pogodin, V. A. Baulin, G. S. Watson, J. A. Watson, R. J. Crawford and E. P. Ivanova, Selective bactericidal activity of nanopatterned superhydrophobic cicada Psaltoda claripennis wing surfaces, *Appl. Microbiol. Biotechnol.*, 2013, **97**(20), 9257–9262.

68 E. P. Ivanova, J. Hasan, H. K. Webb, G. Gervinskas, S. Juodkazis, V. K. Truong, A. H. Wu, R. N. Lamb, V. A. Baulin and G. S. Watson, Bactericidal activity of black silicon, *Nat. Commun.*, 2013, **4**(1), 1–7.

69 A. Kramer, I. Schwebke and G. Kampf, How long do nosocomial pathogens persist on inanimate surfaces? A systematic review, *BMC Infect. Dis.*, 2006, **6**(1), 130.

70 R. A. Weinstein and B. Hota, Contamination, disinfection, and cross-colonization: are hospital surfaces reservoirs for nosocomial infection?, *Clin. Infect. Dis.*, 2004, **39**(8), 1182–1189.

71 V. Russotto, A. Cortegiani, T. Fasciana, P. Iozzo, S. M. Raineri, C. Gregoretti, A. Giammanco and A. Giarratano, What healthcare workers should know about environmental bacterial contamination in the intensive care unit, *BioMed Res. Int.*, 2017, **2017**, 6905450.